Output Stabilization of Boundary-controlled Parabolic PDEs via Gradient-based Dynamic Optimization*

Zhigang Ren[1], Chao Xu[1], Qun Lin[2], and Ryan Loxton[2]

***Abstract*—This paper proposes a new control synthesis approach for the stabilization of boundary-controlled parabolic partial differential equations (PDEs). In the proposed approach, the optimal boundary control is expressed in integral state feedback form with quadratic kernel function, where the quadratic's coefficients are decision variables to be optimized. We introduce a system cost functional to penalize both state and kernel magnitude, and then derive the cost functional's gradient in terms of the solution of an auxiliary "costate" PDE. On this basis, the output stabilization problem can be solved using gradient-based optimization techniques such as sequential quadratic programming. The resulting optimal boundary control is guaranteed to yield closed-loop stability under mild conditions. The primary advantage of our new approach is that the costate PDE is in standard form and can be solved easily using the finite difference method. In contrast, the traditional control synthesis approaches for boundary-controlled parabolic PDEs (i.e., the LQ control and backstepping approaches) require solving non-standard Riccati-type and Klein-Gorden-type PDEs.**

I. INTRODUCTION

Parabolic partial differential equation (PDE) systems are an important type of distributed parameter system (DPS) describing a wide range of natural phenomena, including diffusion, heat transfer, and fusion plasma transport. Over the past few decades, control theory for the parabolic DPS has developed into a mature research topic at the interface of engineering and applied mathematics [1], [2], [10].

The linear quadratic (LQ) control framework is well-defined in infinite dimensional function spaces to deal with the parabolic DPS (e.g., [1], [2]). However, the LQ control framework requires solving Riccati-type differential equations, which are nonlinear parabolic PDEs of dimension one greater than the original parabolic PDE system. For example, to generate an optimal feedback controller for a scalar heat equation, a Riccati PDE defined over a rectangular domain must be solved [11]. Hence, the LQ approach does not actually solve the controller synthesis problem directly, but instead converts it into another problem (i.e., solve a Riccati-type PDE) that is still extremely difficult to solve from a computational point of view.

*This work was supported by the National Natural Science Foundation of China (grants F030119-61104048 and 61320106009) and the National High Technology Research and Development Program of China (grant 2012AA041701)

[1]Z. Ren and C. Xu are with the State Key Laboratory of Industrial Control Technology and the Institute of Cyber-Systems & Control, Zhejiang University, Hangzhou, China. renzhigang@zju.edu.cn, cxu@zju.edu.cn

[2]Q. Lin and R. Loxton are with the Department of Mathematics & Statistics, Curtin University, Perth, Australia. q.lin@curtin.edu.au, r.loxton@curtin.edu.au

Correspondence to: cxu@zju.edu.cn

One of the major advances in PDE control in recent years has been the so-called infinite dimensional Voltera integral feedback, or the backstepping method (e.g., [5], [9]). Instead of Riccati-type PDEs, the backstepping method requires solving the so-called kernel equations—linear Klein-Gorden-type PDEs for which the successive approach can be used to obtain explicit solutions. This method was originally developed for the stabilization of one dimensional parabolic DPS and then extended to fluid flows [16], [19], magnetohydrodynamic flows [17], and elastic vibration [4]. In addition, the backstepping method can also be applied to achieve full state feedback stabilization and state estimation of PDE-ODE cascade systems [13].

In this paper, we propose a new framework for control synthesis for boundary-controlled parabolic DPS. This new framework does not require solving Riccati-type or Klein-Gorden-type PDEs. Instead, it requires solving a so-called "costate" PDE, which is much easier to solve from a computational viewpoint. In fact, many numerical software packages, such as Comsol Multiphysics and MATLAB PDE ToolBox, can be used to generate numerical solutions for the costate PDE. The Riccati PDEs, on the other hand, are usually not in standard form and thus cannot be solved using off-the-shelf software packages. The approach proposed in this paper can be viewed as an extension of optimization-based PID tuning ideas (see [3], [6], [14], [18]) to infinite dimensional systems.

II. PROBLEM FORMULATION

A. Feedback Kernel Optimization

We consider the following parabolic PDE system:

$$\begin{cases} y_t(x,t) = y_{xx}(x,t) + cy(x,t), & \text{(1a)} \\ y(0,t) = 0, & \text{(1b)} \\ y(1,t) = u(t), & \text{(1c)} \\ y(x,0) = y_0(x), & \text{(1d)} \end{cases}$$

where $c > 0$ is a given constant and $u(t)$ is a boundary control. It is well known that the uncontrolled version of system (1) is unstable when the constant c is sufficiently large [5]. According to the LQ control [11] and backstepping synthesis approaches [5], the optimal stabilizing control law takes the following feedback form:

$$u(t) = \int_0^1 \mathscr{K}(1,\xi) y(\xi,t) d\xi, \qquad (2)$$

where the feedback kernel $\mathscr{K}(1,\xi)$ is obtained by solving either a Riccati-type or a Klein-Gorden-type PDE. By introducing the new notation $k(\xi) = \mathscr{K}(1,\xi)$, we can write the

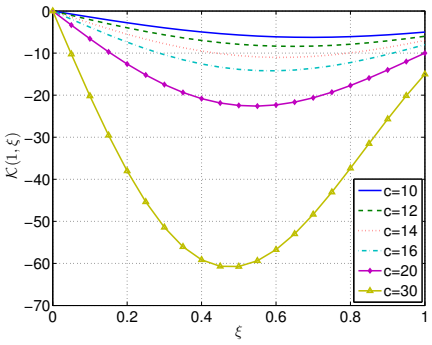

Fig. 1. The feedback kernel (4) for various values of c.

feedback control policy (2) in the following form:

$$u(t) = \int_0^1 k(\xi) y(\xi,t) d\xi.$$

The corresponding closed-loop system is

$$\begin{cases} y_t(x,t) = y_{xx}(x,t) + cy(x,t), & \text{(3a)} \\ y(x,0) = y_0(x), & \text{(3b)} \\ y(0,t) = 0, & \text{(3c)} \\ y(1,t) = \int_0^1 k(\xi) y(\xi,t) d\xi. & \text{(3d)} \end{cases}$$

In reference [5], the backstepping method is used to express the optimal feedback kernel as follows:

$$\mathscr{K}(1,\xi) = -c\xi \frac{I_1(\sqrt{c(1-\xi^2)})}{\sqrt{c(1-\xi^2)}}, \tag{4}$$

where I_1 is the first-order modified Bessel function given by

$$I_1(\omega) = \sum_{n=0}^{\infty} \frac{\omega^{2n+1}}{2^{2n+1} n!(n+1)!}.$$

The feedback kernel (4) is plotted in Figure 1 for different values of c. Note that its shape is similar to a quadratic function. Note also that $\mathscr{K}(1,\xi) = 0$ when $\xi = 0$. Accordingly, motivated by the quadratic behavior exhibited in Fig. 1, we express $k(\xi)$ in the following parameterized form:

$$k(\xi;\Theta) = \theta_1 \xi + \theta_2 \xi^2, \tag{5}$$

where $\Theta = (\theta_1, \theta_2)^\top$ is a parameter vector to be optimized.

Moreover, we assume that the parameters must satisfy the following bound constraints:

$$a_1 \le \theta_1 \le b_1, \quad a_2 \le \theta_2 \le b_2, \tag{6}$$

where a_1, a_2, b_1 and b_2 are given bounds.

Let $y(x,t;\Theta)$ denote the solution of the closed-loop system (3) with the parameterized kernel (5). The results in [15] ensure that such a solution exists and is unique. Our goal is to stabilize the closed-loop system with minimal energy input. Accordingly, we consider the following cost functional:

$$g_0(\Theta) = \frac{1}{2}\int_0^T \int_0^1 y^2(x,t;\Theta) dx dt + \frac{1}{2}\int_0^1 k^2(x;\Theta) dx. \tag{7}$$

We now state our kernel optimization problem formally as follows.

Problem 2.1: Given the PDE system (3) with the parameterized kernel (5), find an optimal parameter vector $\Theta = (\theta_1, \theta_2)^\top$ such that the cost functional (7) is minimized subject to the bound constraints (6).

B. Closed-Loop Stability

Since (7) is a finite-time cost functional, there is no guarantee that the optimized kernel (5) generated by the solution of Problem 2.1 stabilizes the closed-loop system (3) as $t \to \infty$. Nevertheless, we now show that, by analyzing the solution structure of (3), additional constraints can be added to Problem 2.1 to ensure closed-loop stability.

Using the separation of variables approach, we decompose $y(x,t)$ as follows:

$$y(x,t) = \mathscr{X}(x)\mathscr{T}(t). \tag{8}$$

Substituting (8) into (3a), we obtain

$$\mathscr{X}(x)\dot{\mathscr{T}}(t) = \mathscr{X}''(x)\mathscr{T}(t) + c\mathscr{X}(x)\mathscr{T}(t), \tag{9}$$

where

$$\dot{\mathscr{T}}(t) = \frac{d\mathscr{T}(t)}{dt}, \quad \mathscr{X}''(x) = \frac{d^2\mathscr{X}(x)}{dx^2}.$$

Furthermore, from the boundary conditions (3c) and (3d),

$$\mathscr{X}(0)\mathscr{T}(t) = 0,$$
$$\mathscr{X}(1)\mathscr{T}(t) = \int_0^1 k(\xi;\Theta)\mathscr{X}(\xi)\mathscr{T}(t) d\xi.$$

Thus, we immediately obtain

$$\mathscr{X}(0) = 0, \tag{10}$$

$$\mathscr{X}(1) = \int_0^1 k(\xi;\Theta)\mathscr{X}(\xi) d\xi. \tag{11}$$

Rearranging (9) gives

$$\frac{\mathscr{X}''(x) + c\mathscr{X}(x)}{\mathscr{X}(x)} = \frac{\dot{\mathscr{T}}(t)}{\mathscr{T}(t)} = \sigma, \tag{12}$$

where σ is a constant called the eigenvalue. Clearly,

$$\mathscr{T}(t) = T_0 e^{\sigma t}, \tag{13}$$

where $T_0 = \mathscr{T}(0)$ is a constant to be determined.

To solve for $\mathscr{X}(x)$, we must consider three cases: (i) $c < \sigma$; (ii) $c = \sigma$; (iii) $c > \sigma$. In cases (i) and (ii), the general solutions of (12) are, respectively,

$$\mathscr{X}(x) = X_0 e^{\sqrt{\sigma - c}x} + X_1 e^{-\sqrt{\sigma - c}x},$$

and

$$\mathscr{X}(x) = X_0 + X_1 x,$$

where X_0 and X_1 are constants to be determined from the boundary conditions (10) and (11). Then the corresponding solutions of (3) are

$$y(x,t) = X_0 T_0 e^{\sqrt{\sigma - c}x + \sigma t} + X_1 T_0 e^{-\sqrt{\sigma - c}x + \sigma t},$$

and

$$y(x,t) = X_0 T_0 e^{\sigma t} + X_1 T_0 x e^{\sigma t}.$$

These solutions are clearly unstable because $0 < c \leq \sigma$. Thus, the parameters θ_1 and θ_2 should be chosen so that the unique solution of (3) satisfies case (iii) instead of cases (i) and (ii).

In case (iii), the general solution of (12) is

$$\mathscr{X}(x) = X_0 \cos(\sqrt{c-\sigma}x) + X_1 \sin(\sqrt{c-\sigma}x), \qquad (14)$$

where X_0 and X_1 are constants to be determined from the boundary conditions (10) and (11). Substituting (14) into (10), we obtain

$$\mathscr{X}(0) = X_0 = 0.$$

Hence,

$$\mathscr{X}(x) = X_1 \sin(\sqrt{c-\sigma}x). \qquad (15)$$

To simplify the notation, we introduce a new variable $\alpha = \sqrt{c-\sigma}$. Substituting (15) into condition (11), we have

$$X_1 \sin\alpha = X_1 \int_0^1 \theta_1 \xi \sin(\alpha\xi) d\xi + X_1 \int_0^1 \theta_2 \xi^2 \sin(\alpha\xi) d\xi,$$

and thus

$$\sin\alpha = \int_0^1 \theta_1 \xi \sin(\alpha\xi) d\xi + \int_0^1 \theta_2 \xi^2 \sin(\alpha\xi) d\xi. \qquad (16)$$

By evaluating the integrals on the right-hand side, equation (16) can be simplified to obtain

$$\begin{aligned}(\theta_1\alpha^2 + \theta_2\alpha^2 - 2\theta_2)\cos\alpha \\ + (\alpha^3 - \theta_1\alpha - 2\theta_2\alpha)\sin\alpha + 2\theta_2 = 0.\end{aligned} \qquad (17)$$

For any α satisfying (17), there exists a corresponding solution of (12) in the form (15). It can be shown that (17) has an infinite number of positive solutions when $\Theta = (\theta_1, \theta_2)^\top$ satisfies the following inequality:

$$\theta_1^2 + \theta_2^2 + 2\theta_1\theta_2 - 2\theta_1 - 4\theta_2 \geq 0.$$

This is demonstrated numerically in Section IV. A formal proof will be given in a forthcoming journal article [12]. Let $\{\alpha_n\}_{n=1}^\infty$ be a sequence of positive solutions of (17). Then the general solution of (12) is

$$\mathscr{X}(x) = \sum_{n=1}^\infty A_n \sin(\alpha_n x),$$

where A_n are constants to be determined. The corresponding eigenvalues are

$$\sigma_n = c - \alpha_n^2, \quad n = 1, 2, 3, \ldots$$

Hence, using (13),

$$y(x,t) = \mathscr{X}(x)\mathscr{T}(t) = \sum_{n=1}^\infty T_0 A_n e^{(c-\alpha_n^2)t} \sin(\alpha_n x). \qquad (18)$$

By virtue of (10) and (11), this solution satisfies the boundary conditions (3c) and (3d). The constants T_0 and A_n must be selected appropriately so that the initial condition (3b) is also satisfied. To ensure stability as $t \to \infty$, each eigenvalue $\sigma_n = c - \alpha_n^2$ in (18) must be negative. Thus, we impose the following constraints on $\Theta = (\theta_1, \theta_2)^\top$:

$$\theta_1^2 + \theta_2^2 + 2\theta_1\theta_2 - 2\theta_1 - 4\theta_2 \geq 0, \qquad (19a)$$

$$c - \alpha^2 \leq -\varepsilon, \qquad (19b)$$

$$\begin{aligned}(\theta_1\alpha^2 + \theta_2\alpha^2 - 2\theta_2)\cos\alpha \\ + (\alpha^3 - \theta_1\alpha - 2\theta_2\alpha)\sin\alpha + 2\theta_2 = 0,\end{aligned} \qquad (19c)$$

where ε is a given positive parameter and α is the smallest positive solution of (17). Note that α here is treated as an additional optimization variable. Constraint (19a) ensures that there are an infinite number of eigenvalues and thus the solution form (18) is valid. Constraints (19b) and (19c) ensure that the largest eigenvalue is negative, thus guaranteeing solution stability. Adding constraints (19) to Problem 2.1 yields the following modified problem.

Problem 2.2: Given the PDE system (3) with the parameterized kernel (5), choose $\Theta = (\theta_1, \theta_2)^\top$ and α such that the cost functional (7) is minimized subject to the bound constraints (6) and the nonlinear constraints (19).

The next result is concerned with the stability of the closed-loop system corresponding to the optimized kernel from Problem 2.2.

Theorem 2.1: Let (Θ^*, α^*) be an optimal solution of Problem 2.2, where α^* is the smallest positive solution of equation (19c) corresponding to Θ^*. Suppose that there exists a sequence $\{\alpha_n^*\}_{n=1}^\infty$ of positive solutions to equation (19c) corresponding to Θ^* such that $y_0(x) \in \text{span}\{\sin(\alpha_n^* x)\}$. Then the closed-loop system (3) corresponding to Θ^* is stable.

Proof: Because of constraint (19a), the solution form (18) with $\alpha_n = \alpha_n^*$ is guaranteed to satisfy (3a), (3c) and (3d). If $y_0(x) \in \text{span}\{\sin(\alpha_n^* x)\}$, then there exists constants $Y_n, n \geq 1$, such that

$$y_0(x) = \sum_{n=1}^\infty Y_n \sin(\alpha_n^* x).$$

Taking $Y_n = T_0 A_n$ ensures that (18) with $\alpha_n = \alpha_n^*$ also satisfies the initial conditions (3b), and is therefore the unique solution of (3). Since α^* is the first positive solution of equation (17), it follows from constraints (19b) and (19c) that for each $n \geq 1$,

$$c - (\alpha_n^*)^2 \leq c - (\alpha^*)^2 \leq -\varepsilon < 0.$$

This shows that all eigenvalues are negative. ■

Theorem 2.1 requires that the initial function $y_0(x)$ be contained within the linear span of sinusoidal functions $\sin(\alpha_n^* x)$, where each α_n^* is a solution of equation (17) corresponding to Θ^*. The good thing about this condition is that it can be verified numerically by solving the following optimization problem: choose span coefficients $Y_n, 1 \leq n \leq N$, to minimize

$$J = \int_0^1 \left| y_0(x) - \sum_{n=1}^N Y_n \sin(\alpha_n^* x) \right|^2 dx, \qquad (20)$$

where N is a sufficiently large integer and each α_n^* is a solution of equation (17) corresponding to the optimal solution of Problem 2.2. If the optimal cost value for this optimization

problem is sufficiently small, then the span condition in Theorem 2.1 is likely to be satisfied, and therefore closed-loop stability is expected. Based on our computational experience, the span condition in Theorem 2.1 is usually satisfied. In fact, as we show in [12], the solutions α_n^* of (17) converge to the integer multiples of π. Thus, it is reasonable to expect that the linear span of $\{\sin(\alpha_n^* x)\}$ is "approximately" the same as the linear span of $\{\sin(n\pi x)\}$, which is known to be a basis for the space of continuous functions defined on $[0,1]$.

III. NUMERICAL COMPUTATION

Problem 2.2 is an optimal parameter selection problem with decision parameters θ_1, θ_2 and α. In principle, such problems can be solved as nonlinear optimization problems using sequential quadratic programming or other nonlinear optimization methods. However, to do this, we need the gradients of the cost functional (7) and the constraint functions (19) with respect to the decision parameters.

Since the constraint functions in (19) are explicit functions of the decision variables, their gradients are easily derived using elementary differentiation. The cost functional (7), on the other hand, is an implicit function of Θ because it depends on the state trajectory $y(x,t)$. Thus, computing the gradient of (7) is a non-trivial task. We now develop a computational method, analogous to the costate method in the optimal control of ordinary differential equations [7], [8], [14], for computing this gradient.

We define the following costate PDE system:

$$\begin{cases} v_t(x,t)+v_{xx}(x,t)+cv(x,t) \\ \qquad +y(x,t;\Theta)-k(x;\Theta)v_x(1,t)=0, & \text{(21a)} \\ v(0,t)=v(1,t)=0, & \text{(21b)} \\ v(x,T)=0. & \text{(21c)} \end{cases}$$

Let $v(x,t;\Theta)$ denote the solution of the costate PDE system (21) corresponding to the parameter vector Θ. Then we have the following theorem.

Theorem 3.1: The gradient of the cost functional (7) is given by

$$\nabla_{\theta_1} g_0(\Theta) = -\int_0^T \int_0^1 x v_x(1,t) y(x,t)\,dx\,dt + \frac{1}{3}\theta_1 + \frac{1}{4}\theta_2,$$
$$\nabla_{\theta_2} g_0(\Theta) = -\int_0^T \int_0^1 x^2 v_x(1,t) y(x,t)\,dx\,dt + \frac{1}{4}\theta_1 + \frac{1}{5}\theta_2,$$

where $y(x,t)=y(x,t;\Theta)$ and $v_x(x,t)=v_x(x,t;\Theta)$.

Proof: For simplicity, we write $y(x,t;\Theta)$ as $y(x,t)$ and $k(x;\Theta)$ as $k(x)$. Let $\psi(x,t)$ be an arbitrary function satisfying

$$\psi(x,T)=0, \quad \psi(0,t)=\psi(1,t)=0. \tag{22}$$

Then we can rewrite the cost functional (7) in augmented form as follows:

$$g_0(\Theta) = \frac{1}{2}\int_0^T \int_0^1 y^2(x,t)\,dx\,dt + \frac{1}{2}\int_0^1 k^2(x)\,dx + \int_0^T \int_0^1 \psi(x,t)\big\{-y_t(x,t)+y_{xx}(x,t)+cy(x,t)\big\}\,dx\,dt. \tag{23}$$

Using integration by parts and applying conditions (3b), (3c) and (22), we can simplify the augmented cost functional (23) to obtain

$$g_0(\Theta) = \frac{1}{2}\int_0^T \int_0^1 y^2(x,t)\,dx\,dt + \frac{1}{2}\int_0^1 k^2(x)\,dx + \int_0^T \int_0^1 \big\{\psi_t(x,t)+\psi_{xx}(x,t)+c\psi(x,t)\big\}y(x,t)\,dx\,dt + \int_0^1 \psi(x,0)y_0(x)\,dx - \int_0^T \psi_x(1,t)y(1,t)\,dt.$$

Now, consider a perturbation $\delta\rho$ in the parameter vector Θ, where δ is a constant of sufficiently small magnitude and ρ is an arbitrary vector. The corresponding perturbation in the state is,

$$y_\delta(x,t) = y(x,t) + \delta\langle\nabla_\Theta y(x,t),\rho\rangle + \mathscr{O}(\delta^2), \tag{24}$$

and the perturbation in the feedback kernel is,

$$k_\delta(x) = k(x) + \delta\langle\nabla_\Theta k(x),\rho\rangle + \mathscr{O}(\delta^2), \tag{25}$$

where $\mathscr{O}(\delta^2)$ denotes omitted second-order terms such that $\delta^{-1}\mathscr{O}(\delta^2)\to 0$ as $\delta\to 0$. For notational simplicity, we define $\eta(x,t)=\langle\nabla_\Theta y(x,t),\rho\rangle$. Obviously, $\eta(x,0)=0$, because the initial profile $y_0(x)$ is independent of the parameter vector Θ. Based on (24) and (25), the perturbed augmented cost functional takes the following form:

$$\begin{aligned} g_0(\Theta+\delta\rho) &= \frac{1}{2}\int_0^T \int_0^1 \big\{y(x,t)+\delta\eta(x,t)\big\}^2\,dx\,dt \\ &+ \int_0^T \int_0^1 \big\{\psi_t(x,t)+\psi_{xx}(x,t)\big\}\big\{y(x,t)+\delta\eta(x,t)\big\}\,dx\,dt \\ &+ \int_0^T \int_0^1 c\psi(x,t)\big\{y(x,t)+\delta\eta(x,t)\big\}\,dx\,dt \\ &- \int_0^T \psi_x(1,t)\left[\int_0^1 k(x)\big\{y(x,t)+\delta\eta(x,t)\big\}\,dx\right]dt \\ &- \int_0^T \psi_x(1,t)\left[\int_0^1 \delta\langle\nabla_\Theta k(x),\rho\rangle y(x,t)\,dx\right]dt \\ &+ \frac{1}{2}\int_0^1 \big\{k(x)+\delta\langle\nabla_\Theta k(x),\rho\rangle\big\}^2\,dx \\ &+ \int_0^1 \psi(x,0)y_0(x)\,dx + \mathscr{O}(\delta^2). \end{aligned} \tag{26}$$

Taking the derivative of (26) with respect to δ and setting $\delta=0$ gives

$$\begin{aligned} \langle\nabla_\Theta g_0(\Theta),\rho\rangle &= \left.\frac{dg_0(\Theta+\delta\rho)}{d\delta}\right|_{\delta=0} \\ &= \int_0^T \int_0^1 \big\{y(x,t)+\psi_t(x,t)+\psi_{xx}(x,t)+c\psi(x,t)\big\}\eta(x,t)\,dx\,dt \\ &- \int_0^T \int_0^1 \psi_x(1,t)k(x)\eta(x,t)\,dx\,dt \\ &- \int_0^T \int_0^1 \psi_x(1,t)\langle\nabla_\Theta k(x),\rho\rangle y(x,t)\,dx\,dt \\ &+ \int_0^1 k(x)\langle\nabla_\Theta k(x),\rho\rangle\,dx. \end{aligned}$$

Since the perturbation ρ was selected arbitrarily, the theorem follows immediately by setting $\psi(x,t)=v(x,t;\Theta)$ and taking

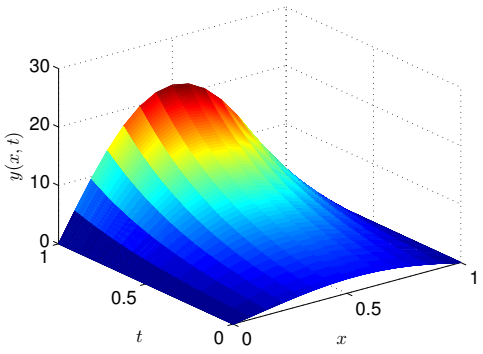

Fig. 2. Uncontrolled open-loop response.

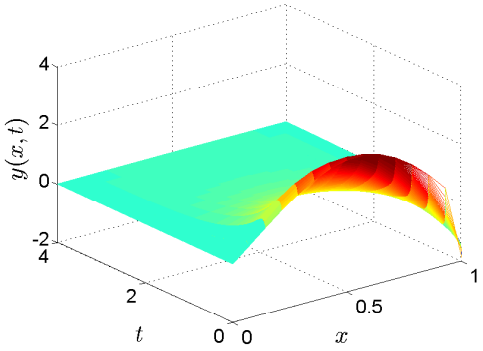

Fig. 3. Optimal closed-loop response.

ρ to be the standard unit basis vectors in $\mathbb{R}^2$. This completes the proof. ■

By combining the gradient formulas in Theorem 3.1 with a standard gradient-based optimization method (such as sequential quadratic programming), Problem 2.2 can be solved efficiently.

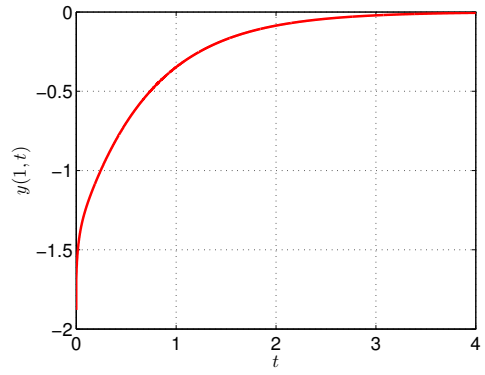

Fig. 4. Optimal boundary control.

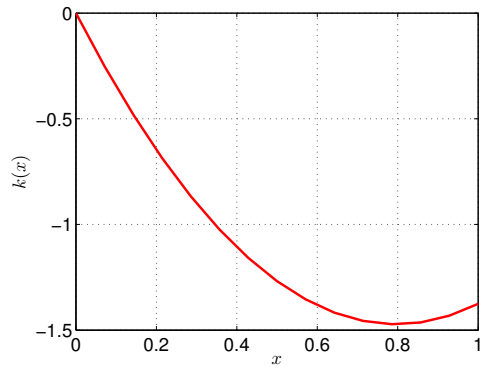

Fig. 5. Optimal kernel function.

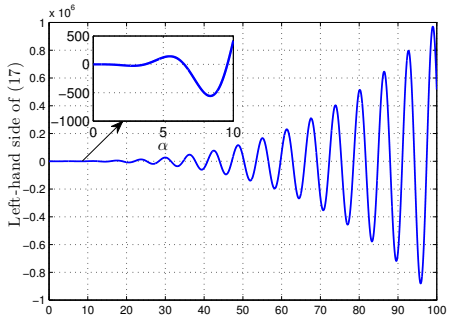

Fig. 6. Equation (17) has an infinite number of positive solutions.

IV. NUMERICAL EXAMPLE

We consider Problem 2.2 over a time horizon of $[0,T] = [0,4]$. To solve the problem, we wrote a MATLAB program that combines the FMINCON optimization function with the gradient formulas in Theorem 3.1. The state system (3) and the costate system (21) are solved numerically using the finite difference method (with 14 spatial intervals and 5000 temporal intervals). All numerical simulations were performed on a desktop computer with the following configuration: Intel Core i7-2600 3.40GHz CPU, 4.00GB RAM, 64-bit Windows 7 Operating System.

Consider the uncontrolled version of (3) in which $u(t) = 0$. In this case, the exact solution is [5]

$$y(x,t) = 2\sum_{n=1}^{\infty} C_n e^{(c-n^2\pi^2)t}\sin(n\pi x)dx, \qquad (27)$$

where C_n are the Fourier coefficients defined by

$$C_n = \int_0^1 y_0(x)\sin(n\pi x)dx.$$

The eigenvalues of (27) are $c-n^2\pi^2$, $n = 1,2,\ldots$ The largest eigenvalue is therefore $c-\pi^2$, which indicates that system (3) with $u(t) = 0$ is unstable for $c > \pi^2 \approx 9.8696$.

We choose $c = 12$ and $y_0(x) = (2+x)\sin(\pi x)$. The corresponding uncontrolled open-loop response (see equation (27)) is shown in Fig. 2. As we can see from Fig. 2, the state

TABLE I
SOLUTIONS OF EQUATION (17) AND CORRESPONDING SPAN COEFFICIENTS.

n	α_n^*	α_n^*/π	Y_n
1	3.6934	1.0801	−0.4211
2	6.4961	2.0678	1.5226
3	9.5794	3.0492	1.4629
4	12.6751	4.0346	−0.7636
5	15.7975	5.0285	0.4483
6	18.9223	6.0231	−0.3458
7	22.0544	7.0201	0.2681
8	25.1874	8.0173	0.9085
9	28.3233	9.0155	1.0726
10	31.4597	10.0139	0.9415
11	34.5975	11.0127	1.0418
12	37.7356	12.0116	0.9709
13	40.8745	13.0107	1.0156
14	44.0136	14.0099	0.9968
15	47.1532	15.0093	0.9908

of the uncontrolled system grows as time increases. For the feedback kernel optimization, we suppose that the lower and upper bounds for the optimization parameters are $a_i = -10$ and $b_i = 10$, respectively. We also choose $\varepsilon = 1$ in (19b). Starting from the initial guess $(\theta_1, \theta_2, \alpha) = (-1, 2, 0)$, our program terminates after 29 iterations and 21.0904 seconds. The optimal cost value is $g_0 = 1.2092$ and the optimal solution of Problem 2.2 is $(\theta_1^*, \theta_2^*, \alpha^*) = (-3.6977, 2.3220, 3.6934)$.

The spatial-temporal response of the controlled plant corresponding to (θ_1^*, θ_2^*) is shown in Fig. 3. The figure clearly shows that the controlled system (3) with optimized parameters (θ_1^*, θ_2^*) is stable. The corresponding optimal boundary control and kernel function are shown in Fig. 4 and Fig. 5, respectively.

Recall from Theorem 2.1 that closed-loop stability is guaranteed if $\alpha^* = 3.6934$ is the first positive solution of equation (17) and the initial function $y_0(x)$ is contained within the linear span of $\{\sin(\alpha_n^* x)\}$, where each α_n^* is a solution of equation (17) corresponding to (θ_1^*, θ_2^*). By viewing a plot of the left-hand side of equation (17), it can be easily verified that α^* is indeed the first positive solution; see Fig. 6. To verify the linear span condition, we use FMINCON in MATLAB to minimize (20) for $N = 20$. The first 15 positive solutions of (17) corresponding to the optimal parameters $\theta_1^* = -3.6977$ and $\theta_2^* = 2.3220$ are given in Table I. The optimal span coefficients that minimize (20) are also given. The optimal value of J in (20) is 7.7387×10^{-14}, which indicates that the span condition holds. Note also from Table I that α_n^*/π converges to an integer as $n \to \infty$.

V. CONCLUSIONS

In this paper, we have introduced a new gradient-based optimization approach for boundary stabilization of parabolic PDE systems. Our new approach involves expressing the boundary controller as an integral state feedback in which a kernel function needs to be designed judiciously. We do not determine the feedback kernel by solving Riccati-type or Klein-Gorden-type PDEs; instead, we approximate the feedback kernel by a quadratic function and then optimize the quadratic's coefficients using dynamic optimization techniques. This preliminary work has also raised several issues that require further investigation: (i) Can the proposed kernel optimization approach be applied to other classes of PDE plant models (i.e., 2D or 3D domains)? (ii) Is it possible to develop methods for minimizing cost functional (7) over an infinite time horizon? These issues will be explored in future work.

REFERENCES

[1] A. Bensoussan, G. Da Prato, M. C. Delfour and S. K. Mitter, "Representation and Control of Infinite Dimensional Systems", Birkhauser, Boston, 2007.

[2] R. F. Curtain and H. Zwart, "An Introduction to Infinite-dimensional Linear Systems Theory", Springer, New York, 1995.

[3] N. J. Killingsworth and M. Krstic, "PID tuning using extremum seeking: Online, model-free performance optimization", *IEEE Control Systems Magazine,* vol. 26, no. 1, pp. 70-79, 2006.

[4] M. Krstic, B. Guo, A. Balogh and A. Smyshlyaev, "Control of a tip-force destabilized shear beam by observer-based boundary feedback", *SIAM Journal on Control and Optimization,* vol. 47, no. 2, pp. 553-574, 2008.

[5] M. Krstic and A. Smyshlyaev, "Boundary Control of PDEs: A Course on Backstepping Designs", SIAM, Philadelphia, 2008.

[6] B. Li, K. L. Teo, C. Lim and G. Duan, "An optimal PID controller design for nonlinear constrained optimal control problems", *Discrete and Continuous Dynamical Systems – Series B,* vol. 16, no. 4, pp. 70-79, 2011.

[7] Q. Lin, R. Loxton and K. L. Teo, "Optimal control of nonlinear switched systems: Computational methods and applications", *Journal of the Operations Research Society of China,* vol. 1, no. 3, pp. 275-311, 2013.

[8] Q. Lin, R. Loxton and K. L. Teo, "The control parameterization method for nonlinear optimal control: A survey", *Journal of Industrial and Management Optimization,* vol. 10, no. 1, pp. 275-309, 2014.

[9] W. Liu, "Boundary feedback stabilization of an unstable heat equation", *SIAM Journal on Control and Optimization,* vol. 42, no. 3, pp. 1033-1043, 2003.

[10] W. Liu, "Elementary Feedback Stabilization of the Linear Reaction-convection-diffusion Equation and the Wave Equation", Springer, Berlin, 2010.

[11] S. J. Moura and H. K. Fathy, "Optimal boundary control of reaction-diffusion partial differential equations via weak variations", *Journal of Dynamic Systems, Measurement, and Control,* vol. 135, no. 3, 034501(1-8), 2013.

[12] Z. Ren, C. Xu, Q. Lin and R. Loxton, "A gradient-based kernel optimization approach for parabolic distributed parameter control systems", *Pacific Journal of Optimization,* accepted.

[13] G. A. Susto and M. Krstic, "Control of PDE-ODE cascades with Neumann interconnections", *Journal of the Franklin Institute,* vol. 347, no. 1, pp. 284-314, 2010.

[14] K. L. Teo, C. J. Goh and K. H. Wong, "A Unified Computational Approach to Optimal Control Problems", Longman Scientific and Technical, Essex, 1991.

[15] R. Triggiani, "Well-posedness and regularity of boundary feedback parabolic systems", *Journal of Differential Equations,* vol. 36, no. 3, pp. 347-362, 1980.

[16] R. Vazquez and M. Krstic, "A closed-form feedback controller for stabilization of the linearized 2-D Navier-Stokes Poiseuille system", *IEEE Transactions on Automatic Control,* vol. 52, no. 12, pp. 2298-2312, 2007.

[17] R. Vazquez and M. Krstic, "Control of Turbulent and Magnetohydrodynamic Channel Flows: Boundary Stabilization and State Estimation", Springer, Boston, 2008.

[18] J. Xu, D. Huang and S. Pindi, "Optimal tuning of PID parameters using iterative learning approach", *SICE Journal of Control, Measurement, and System Integration,* vol. 1, no. 3, pp. 143-154, 2008.

[19] C. Xu, E. Schuster, R. Vazquez and M. Krstic, "Stabilization of linearized 2D magnetohydrodynamic channel flow by backstepping boundary control", *Systems & Control Letters,* vol. 57, no. 10, pp. 805-812, 2008.

Optimal Power Allocation for Non-Regenerative Multicarrier Relay-Assisted PLC Systems with QoS Constraints

Xiaolin Wu
Department of Electrical and Computer Engineering
Curtin University of Technology
Perth, WA 6102, Australia
Email:xiaolin.wu@curtin.edu.au

Yue Rong
Department of Electrical and Computer Engineering
Curtin University of Technology
Perth, WA 6102, Australia
Email:Y.Rong@curtin.edu.au

***Abstract*—In this paper we present an iterative algorithm to jointly optimize the source and relay power allocations for a general relay transmission system, i.e. the broadcast-and-multiaccess (BMA) multicarrier relay system, where the source transmits in two time-slots. Under the indoor power line communication environment, we examine the issue of minimization of the total network transmission power subjecting to QoS constraints expressed as the capacity lower-bound of the data-link from the source to the destination nodes. In addition to demonstrate the fast convergence of the proposed algorithm, the simulation results also show that with respect to the two-hop relay system and the broadcast-and-forward (BF) relay system, the proposed general relay system can satisfy the same QoS requirement while consume less total transmission power.**

***Index Terms*—Power Line Communications (PLC), multi-carrier relay, time varying channel, three-node system, non-regenerative relay, QoS.**

I. Introduction

Indoor power line communication (PLC) technology has received much research attention. In addition to electricity delivery, the indoor power cables are used as medium, at the meantime, to support local area networks (LAN). However, as the indoor power cables are not manufactured for high frequency (HF) signal transmission purpose, indoor PLC channels have demonstrated hostile characteristics for broadband communications. Due to the similar broadcasting nature between the wireless signal propagation and the power-cable guided signal transmission, some advanced relay schemes can be readily introduced into PLC systems. However, [1] pointed out a notable difference between PLC relay channels and the wireless relay systems. In wireless systems the source-to-destination, source-to-relay and relay-to-destination paths can be considered as independent to each other so that the spatial diversity gain can be achieved. On the other hand, in PLC environment these paths are highly correlated, as they share the same power cable grid all the time. The authors of [2] have investigated the optimal time-slot duration allocation between the direct transmission phase and the relay phase, when there is only one relay node. Under the assumption that each outlet on the power grid is a potential relay node, [3] proposed a multi-hop transmission scheme combined with the application of distributed space-time block code (DSTBC) in PLC networks.

Depending on the signal processing type used in the relay node, relay schemes can be classified into two groups, namely regenerative and non-regenerative relay systems. As the non-regenerative scheme only requires the relay node amplify-and-forward (AF) signals, it has lower complexity, shorter processing delay and lower implementation cost. In [4] algorithms have been developed to maximize the relay system throughput by assuming that the relay works in non-regenerative mode and the powers at the source node and the relay node can be distributed over multiple sub-carriers. The communication process is completed in two successive phases. In the first phase, the source node transmits signal to the relay node. In the second phase, the relay node amplifies each sub-carrier component of the signal received from the source node, and forward the amplified signals to the destination node. We call this *two-hop* relay scheme as there is no direct path between the source and destination nodes. The effect of the direct link has been considered in [5], [6], where in the first phase the source broadcasts signal to the relay and destination nodes. In the second phase, the relay forwards its received signal to the destination. As a result, the source node is always silent during the second phase. We call this *broadcast-and-forward* (BF) relay scheme. In [7] the authors took another step that they allow the source to transmit in both the first and second phases. In other words, when the relay node forwards its received signal, the source repeat a transmission of the same information (as in the first phase) to the destination in the second phase. We refer this as *broadcast-and-multiaccess* (BMA) relay scheme. As a result of this configuration, the total network transmission power has been separated into relay power and source power, which in turn has been split into two part (corresponding to two phases) for transmitting the same information twice. Obviously this is a very general case comparing with the above two-hop and BF schemes.

In the conventional direct transmission (DT) system, the rate

maximization (RM) and margin maximization (MM) problems are of duality to each other and admit a unique water-filling solution [8]. However this fact does not hold when relay node has been introduced. The aim of [4], [5], [6], [7] is to optimize a given objective function, usually expressed as signal-to-noise ratio (SNR), mutual information (MI) or system capacity, subjecting to the power constraints of the whole network or/and at each node. On the other hand, the quality-of-service (QoS) constraints are not addressed. Note that in practical indoor PLC applications, such as HD Video Streaming, QoS criteria is very important as they greatly affect the user experience.

In this paper we address the joint optimization of source and relay power allocation to minimize the total network consuming power subjecting to QoS constraints, which has not been considered before. We set the QoS criteria as the lower-bound of the capacity of the data-link from the source to the destination node. Since the QoS-constrained power allocation problem is highly non-convex, the globally optimal solution is computationally intractable to obtain. To overcome this challenge, we propose an alternating optimization (AO) method adapted from [9] to decompose the joint optimization problem into three sub-problems. Simulation results show the fast convergence and short delay of the proposed algorithm.

The remainder of this paper is organized as follows. Section II describes in detail the system model and problem formulation. The decomposed three sub-problems from Section II have been fully discussed in Sections III, IV and V, respectively. Based on these, the overall AO algorithm has been presented in Section VI. Simulation examples are given in Section VII to demonstrate the fast convergence and superior performance of the proposed algorithm. Finally, conclusions are given in Section VIII.

II. System Model and Problem Formulation

The block diagram of the three-node relay system is shown in Fig. 1, which consists of three nodes, i.e. the source node (S), the destination node (D) and the relay node (R). Under a practical topology of indoor power lines this arrangement, every pair of outlets/sockets can be employed as a point-to-point communication system, and its corresponding channel transfer function H_{SD} is characterized by the wiring topology and load impedance between the transceivers. Let us refer to the shortest link between the source and destination nodes as the main path, while other wirings are as treated as tap-brunches attached to the main path, which contribute to the multi-path fading effect of the channel. Any outlet located on the main path or on a brunch of the main path can be chosen to deploy the relay node. Let us also denote the transfer function of the channel transfer function of source-to-relay link and relay-to-destination link as H_{SR} and H_{RD}, respectively. If the relay node has been chosen on the main path, then from the relay node's point of view the whole direct channel has been separated into two parts, thus we can write [1]

$$H_{SD} = H_{SR}H_{RD}. \tag{1}$$

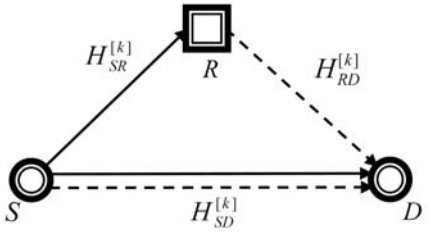

Fig. 1: A multicarrier three-node relay system, where the solid-lines and dash-lines indicate phase 1 and 2, respectively. S, R and D stand for source node, relay node and destination node respectively. $k = 1, \ldots, K$ is the index of sub-carriers.

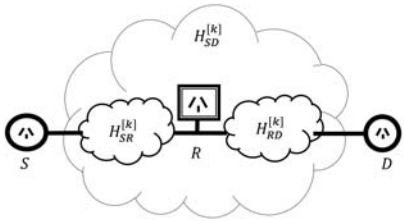

Fig. 2: Channel separation from a relay node's point of view.

This relation has been illustrated in Fig. 2. However, we mention that if the relay node is chosen on a tap-brunch, the relation in (1) does not hold in general.

We consider an orthogonal frequency-division multiplexing (OFDM) based mutlticarrier system. The whole system bandwidth is divided uniformly into K subcarriers, where the channel fading on each subcarrier is considered to be frequency-flat, i.e. it can be described as a channel coefficient. The channel response on the kth ($k = 1, 2, \ldots K$) subcarrier from node L_1 to node L_2 is denoted as $H_{L_1L_2}^{[k]}$, where $L_1 \in \{S, R\}$ and $L_2 \in \{R, D\}$. Let us denote the transmit power on the kth subcarrier from the source node as $P_S^{[k]}$, and from the relay node as $P_R^{[k]}$. Furthermore, to distinguish the source power used in the first and second phase, we denote them as $P_{S,1}^{[k]}$ and $P_{S,2}^{[k]}$ respectively, i.e. $P_S^{[k]} = P_{S,1}^{[k]} + P_{S,2}^{[k]}$. Thus, the total network power P_Σ can be expressed as

$$\begin{aligned} P_\Sigma &= \sum_{k=1}^{K} P_S^{[k]} + \sum_{k=1}^{K} P_R^{[k]} \\ &= \sum_{k=1}^{K} P_{S,1}^{[k]} + \sum_{k=1}^{K} P_{S,2}^{[k]} + \sum_{k=1}^{K} P_R^{[k]}. \end{aligned} \tag{2}$$

Following OFDM principle, corresponding to the K subcarriers, each packet of information is encoded into K independent complex symbols $X^{[k]}$ ($k = 1, 2, \ldots K$), of zero mean and unit variance. To complete a packet of information transmission from the source to the destination, the broadcast-and-multiaccess relay scheme works as the following two phases.

In the first phase, the source node broadcasts information signal $X^{[k]}$ ($k = 1, 2, \dots K$) over the kth subcarrier with the power $P_{S,1}^{[k]}$. Due to the broadcast nature of power line grids, both the relay and the destination can receive this signal with different channel gain and noise disturbances respectively as

$$Y_{R,1}^{[k]} = H_{SR}^{[k]}\sqrt{P_{S,1}^{[k]}}X^{[k]} + N_{R,1}^{[k]} \quad (3)$$

$$Y_{D,1}^{[k]} = H_{SD}^{[k]}\sqrt{P_{S,1}^{[k]}}X^{[k]} + N_{D,1}^{[k]} \quad (4)$$

where $Y_{L_2,n}^{[k]}$and $N_{L_2,n}^{[k]}$ respectively denote the received signal and noise at the node $L_2(L_2 \in \{R, D\})$ in the nth (n =1 or 2) phase.

In the second phase, the relay amplifies its received signals on each sub-carrier, i.e. $Y_{R,1}^{[k]}$, with proper complex gain $g^{[k]}\exp(j\theta^{[k]})$, where $g^{[k]}$ is the amplitude gain and $\theta^{[k]}$ is the phase shift, and then forwards the amplified signals to the destination with power $P_R^{[k]}$. At the meantime, the source node sends another identical message packet out, this time with power $P_{S,2}^{[k]}$. Then the received signal at the destination node in the second phase is

$$\begin{aligned} Y_{D,2}^{[k]} &= H_{RD}^{[k]}g^{[k]}\exp(j\theta^{[k]})Y_{R,1}^{[k]} \\ &\quad + H_{SD}^{[k]}\sqrt{P_{S,2}^{[k]}}X^{[k]} + N_{D,2}^{[k]} \end{aligned} \quad (5)$$

where

$$g^{[k]} = \sqrt{\frac{P_R^{[k]}}{P_{S,1}^{[k]}|H_{SR}^{[k]}|^2 + W_R^{[k]}}} \quad (6)$$

$$\theta^{[k]} = \angle H_{SD}^{[k]} - \angle H_{SR}^{[k]} - \angle H_{RD}^{[k]}. \quad (7)$$

Here we used $W_{L_2}^{[k]}$ to denote the power of noise $N_{L_2,n}^{[k]}$(n =1 or 2) in (6), and $\angle(\cdot)$ stands for the angle of a complex number in (7).

Finally, the destination combines the two copies of received signal (4) and (5) over two phases by maximum ratio combination (MRC) processing with the knowledge of channel state information (CSI). By denoting the SNR of the kth subcarrier at the destination in the nth phase as $SNR_{D,n}^{[k]}$, from (3)-(7) we have

$$SNR_{D,1}^{[k]} = P_{S,1}^{[k]}\gamma_{SD}^{[k]} \quad (8)$$

$$SNR_{D,2}^{[k]} = \frac{\left(\sqrt{P_{S,1}^{[k]}\gamma_{SR}^{[k]}P_R^{[k]}\gamma_{RD}^{[k]}} + \sqrt{P_{S,2}^{[k]}\gamma_{SD}^{[k]}\left(1+P_{S,1}^{[k]}\gamma_{SR}^{[k]}\right)}\right)^2}{1+P_{S,1}^{[k]}\gamma_{SR}^{[k]}+P_R^{[k]}\gamma_{RD}^{[k]}} \quad (9)$$

where the normalized gain of the channel from L_1 to L_2 is introduced as $\gamma_{L_1L_2}^{[k]} = \frac{|H_{L_1L_2}^{[k]}|^2}{W_{L_2}^{[k]}}$. Thus, we obtain the capacity (in bit/sec/Hz) of the data-link from S to D as

$$C = \frac{1}{2}\sum_{k=1}^{K}\log_2\left(1 + SNR_{D,1}^{[k]} + SNR_{D,2}^{[k]}\right) \quad (10)$$

where the factor 1/2 reflects the half-duplex constraint of the relay node.

We note that (10) is the capacity of a general two-phase relay system, which includes the following special cases: (a) If $\gamma_{SD}^{[k]} = 0$, the system becomes a two-hop relay system without the direct link. In PLC scenario this usually happens when the cable length between the source and the destination outlets is very far. (b) If $P_{S,2}^{[k]} = 0$, it means the system becomes a broadcast-and-forward relay system as we mentioned in Section I. (c) Interestingly, if $P_R^{[k]} = 0$, it means the relay node is not active, then the system become a *two-phase direct transmission system*, where the source transmits the same information packet twice independently in two phases to achieve time-diversity. (d) Especially, if $P_R^{[k]} = 0$ and $P_{S,2}^{[k]} = 0$, the scheme degrades to a conventional direct transmission (DT) system[1]. Without losing generality, we assume all $\gamma_{L_1L_2}^{[k]} > 0$ in the following.

With the QoS criteria as the lower-bound of the system capacity, to explore the most efficient utilization of the system power we propose the following optimization problem

$$\min_{P_{S,1}^{[k]}, P_{S,2}^{[k]}, P_R^{[k]}} \quad P_\Sigma \quad (11)$$

$$s.t. \quad C \geq q, \quad (12)$$

$$P_{S,1}^{[k]}, P_{S,2}^{[k]}, P_R^{[k]} \geq 0, \forall k \quad (13)$$

where (11) is the objective function of the total network transmission power, and $q \geq 0$ is the required minimum link capacity to support certain applications. We can also define the averaged subchannel capacity as $\frac{C}{K}$, so that capacity constraint (12) can be equally expressed as

$$\frac{C}{K} \geq q' \quad (14)$$

where $q' = \frac{q}{K}$ is the requirement of average capacity on each subcarrier.

The exact solution to problem (11)-(13) is difficult to find because the system minimum capacity constraint in (12) is non-convex. In this paper, we provide a locally optimal solution by adopting the AO approach from [9], where we firstly optimize $P_R^{[k]}$ with given $P_{S,1}^{[k]}$ and $P_{S,2}^{[k]}(k = 1, 2, \dots K)$, then optimize $P_{S,1}^{[k]}$ with given $P_{S,2}^{[k]}$ and previously optimized $P_R^{[k]}$, and next we optimize $P_{S,2}^{[k]}$ with previously obtained $P_{S,1}^{[k]}$ and $P_R^{[k]}$. This process is repeated until convergence, i.e. the difference between the P_Σ obtained in two consecutive iterations is less than a preset threshold. For any two groups of fixed power allocation parameters, the resulted sub-problem becomes convex. Based on the method, we will develop the overall algorithm to solve the problem (11)-(13). we discuss these issues in detail from Section III to Section VI.

[1]In this case, the relay's half-duplex factor 1/2 does not exist.

III. Optimal relay power allocation when given source power allocations

For fixed $P_{S,1}^{[k]}$ and $P_{S,2}^{[k]}$ $(k = 1, 2, \dots K)$, problem (11)-(13) becomes

$$\min_{P_R^{[k]}} \quad \sum_{k=1}^{K} P_R^{[k]} \tag{15}$$

$$s.t. \quad \frac{1}{2}\sum_{k=1}^{K} \log_2\left(a_k + \frac{b_k}{d_k P_R^{[k]} + c_k}\right) \geq q \tag{16}$$

$$P_R^{[k]} \geq 0, \forall k \tag{17}$$

where

$$\begin{aligned} a_k &= 1 + P_{S,1}^{[k]}\gamma_{SD}^{[k]} + P_{S,1}^{[k]}\gamma_{SR}^{[k]} \\ b_k &= \left(1 + P_{S,1}^{[k]}\gamma_{SR}^{[k]}\right)\left(P_{S,2}^{[k]}\gamma_{SD}^{[k]} - P_{S,1}^{[k]}\gamma_{SR}^{[k]}\right) \\ c_k &= 1 + P_{S,1}^{[k]}\gamma_{SR}^{[k]} \\ d_k &= \gamma_{RD}^{[k]}. \end{aligned}$$

Let us write down the Karush-Kuhn-Tucker (KKT) conditions to the problem (15)-(17) as, for $\forall k$,

$$1 + \lambda \frac{b_k d_k}{\ln 2 (c_k + d_k P_R^{[k]})(b_k + a_k c_k + a_k d_k P_R^{[k]})} = 0 \tag{18}$$

$$\lambda \left[2q - \sum_{k=1}^{K} \log_2\left(a_k + \frac{b_k}{d_k P_R^{[k]} + c_k}\right)\right] = 0 \tag{19}$$

$$\lambda \geq 0 \tag{20}$$

$$P_R^{[k]} \geq 0 \tag{21}$$

It is easy to notice that the Lagrangian multiplier λ cannot take zero value. In addition, it can be proved that only when $b_k < 0$ while $a_k, c_k, d_k > 0$, the problem (15)-(17) have solution. Under this condition the problem (15)-(17) is convex on $\left\{P_R^{[k]} \mid P_R^{[k]} \geq 0, k = 1, 2, \dots K\right\}$. For fixed $\lambda > 0$, as the left-hand-side (LHS) of (18) is a monotonically increasing function of $P_R^{[k]}$ and the LHS of (19) is a decreasing function of $P_R^{[k]}$, we can use a bi-section search algorithm to solve expressions (18)-(21), which in turn leads us to the solution of problem (15)-(17).

IV. Optimal first-phase source power allocation when given second-phase power and relay power allocations

For given $P_{S,2}^{[k]}$ and $P_R^{[k]}$ $(k = 1, 2, \dots K)$, we now consider the optimization of the source power allocation in the first phase, namely $P_{S,1}^{[k]}$, by solving the problem as

$$\min_{P_{S,1}^{[k]}} \quad \sum_{k=1}^{K} P_{S,1}^{[k]} \tag{22}$$

$$s.t. \quad \frac{1}{2}\sum_{k=1}^{K} \log_2\left(A_k + B_k P_{S,1}^{[k]} + \frac{C_k}{D_k P_{S,1}^{[k]} + E_k}\right) \geq q \tag{23}$$

$$P_{S,1}^{[k]} \geq 0, \forall k \tag{24}$$

where

$$\begin{aligned} A_k &= 1 + P_R^{[k]}\gamma_{RD}^{[k]} + P_{S,2}^{[k]}\gamma_{SD}^{[k]} \\ B_k &= \gamma_{SD}^{[k]} \\ C_k &= -P_R^{[k]}\gamma_{RD}^{[k]}\left(1 + P_R^{[k]}\gamma_{RD}^{[k]} + P_{S,2}^{[k]}\gamma_{SD}^{[k]}\right) \\ D_k &= \gamma_{SR}^{[k]} \\ E_k &= 1 + P_R^{[k]}\gamma_{RD}^{[k]}. \end{aligned}$$

Let us write down the KKT condition to the problem (22)-(24) as, for $\forall k$,

$$\left(A_k + B_k P_{S,1}^{[k]} + \frac{C_k}{E_k + P_{S,1} D_k}\right)\ln 2 + \lambda\left(B_k + \frac{C_k D_k}{\left(E_k + P_{S,1}^{[k]} D_k\right)^2}\right) = 0 \tag{25}$$

$$\lambda\left[2q - \sum_{k=1}^{K} \log_2\left(A_k + B_k P_{S,1}^{[k]} + \frac{C_k}{D_k P_{S,1}^{[k]} + E_k}\right)\right] = 0 \tag{26}$$

$$\lambda \geq 0 \tag{27}$$

$$P_{S,1}^{[k]} \geq 0 \quad . \tag{28}$$

We observe that, for fixed $\lambda > 0$, the LHS of (25) is a monotonically increasing function of $P_{S,1}^{[k]}$ and the LHS of (26) is a decreasing function of $P_{S,1}^{[k]}$. Furthermore, the problem (22)-(24) is only solvable when $C_k < 0$ while $A_K, B_k, D_k, E_k > 0$, and under this condition it is convex on $\left\{P_{S,1}^{[k]} \mid P_{S,1}^{[k]} \geq 0, k = 1, 2, \dots K\right\}$. Thus its solution can be found by using the bi-section search algorithm.

V. Optimal second-phase source power allocation when given first-phase power and relay power allocations

Similarly, based on the optimized $P_{S,1}^{[k]}$ from Section IV and $P_R^{[k]}$ from Section III, we now consider the optimization of the source power allocation in the second phase, i.e. $P_{S,2}^{[k]}$, by solving the problem as

$$\min_{P_{S,2}^{[k]}} \quad \sum_{k=1}^{K} P_{S,2}^{[k]} \tag{29}$$

$$s.t. \quad \frac{1}{2}\sum_{k=1}^{K} \log_2\left(\alpha_k + \beta_k P_{S,2}^{[k]}\right) \geq q \tag{30}$$

$$P_{S,2}^{[k]} \geq 0, \forall k \tag{31}$$

where

$$\begin{aligned} \alpha_k &= 1 + P_{S,1}^{[k]}\gamma_{SD}^{[k]} + \frac{P_{S,1}^{[k]}\gamma_{SR}^{[k]} P_R^{[k]}\gamma_{RD}^{[k]}}{1 + P_{S,1}^{[k]}\gamma_{SR}^{[k]} + P_R^{[k]}\gamma_{RD}^{[k]}} \\ \beta_k &= \frac{P_{S,1}^{[k]}\gamma_{SR}^{[k]}\gamma_{SD}^{[k]} + \gamma_{SD}^{[k]}}{1 + P_{S,1}^{[k]}\gamma_{SR}^{[k]} + P_R^{[k]}\gamma_{RD}^{[k]}}. \end{aligned}$$

Algorithm 1 AO algorithm for proposed problem

1) Use bi-section algorithm with preselected (newly obtained) allocations of source power in two phases to solve (18)-(21) to find a new set of relay power.
2) Use bi-section algorithm with the preselected (newly obtained) second-phase source power and newly obtained relay power to solve (25)-(28) to find a new set of first-phase power.
3) Use bi-section algorithm with newly obtained allocations of relay power and first-phase source power to solve (32)-(35) to find a new set of second-phase source power.
4) If the difference of (11) between two consecutive loops is less than a preset threshold σ, then stop; otherwise, GO TO step 1).

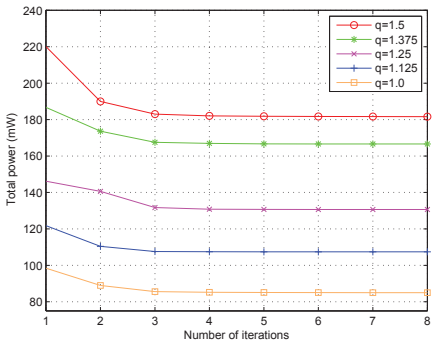

Fig. 3: Total power versus number of iterations.

The KKT conditions to the problem (29)-(31) are, for $\forall k$,

$$1-\lambda\frac{\beta_k}{\ln 2\left(\alpha_k+\beta_k P_{S,2}^{[k]}\right)} = 0 \quad (32)$$

$$\lambda\left[2q-\sum_{k=1}^{K}\log_2\left(\alpha_k+\beta_k P_{S,2}^{[k]}\right)\right] = 0 \quad (33)$$

$$\lambda \geq 0 \quad (34)$$

$$P_{S,2}^{[k]} \geq 0 \quad (35)$$

For fixed $\lambda > 0$, the LHS of (32) is a monotonically increasing function of $P_{S,2}^{[k]}$ and the LHS of (33) is a decreasing function of $P_{S,2}^{[k]}$. Thus, the problem (29)-(31) is solvable and convex on $\left\{P_{S,2}^{[k]} \mid P_{S,2}^{[k]} \geq 0, k=1,2,\ldots K\right\}$, when $a_k, b_k > 0$. Again, its solution can be found by using the bi-section search algorithm.

VI. Proposed Iterative Algorithm

Based on the discussion from Sections III to V, we summarize the proposed AO algorithm, as we mentioned earlier, for solving the proposed problem (11)-(13). This is shown in Algorithm 1.

In general, the alternating optimization method cannot guarantee to converge to the globally optimal solution. However, since constraint in (12) is convex for any fixed group of $\left\{P_{S,1}^{[k]}, P_{S,2}^{[k]}\right\}$, $\left\{P_R^{[k]}, P_{S,2}^{[k]}\right\}$ or $\left\{P_{S,1}^{[k]}, P_R^{[k]}\right\}$, the proposed AO algorithm converges to a stationary point of the objective function (11). This will be verified by the simulation examples in the next section.

VII. Numerical Examples

In this section we present simulation results based on the indoor PLC channel environment by using the direct PLC channel model [11] and noise model [12]. Here, we assume the the relay node has been chosen on the main path, which means with the relation (1) we can cascade two randomly generated direct channel model to get a relay channel. Also, from the randomly generated channel transfer function and noise PSD, we can calculate the normalized channel gain on each subcarrier. For simplicity of presentation, we set the subcarrier amount K as 32, among the usual broadband PLC spectrum, i.e. 2-30MHz. However, we mention that in practical PLC systems this value is usually larger than one thousand. In addition, we set the power spectrum density (PSD) of the noise on the relay node and the destination node to the same, even though this is not always true in the real PLC environment, e.g. an outlet near a noise-generating appliance usually has a stronger PSD than the one which is located further away from that appliance.

For the proposed algorithm, we set the convergence condition as the difference between the total power obtained in two consecutive iterations less than 10^{-5}. As an example to demonstrate the convergence speed of the overall AO algorithm, Fig. 3 shows the total transmission power versus the number of iterations when the averaged subchannel capacity in (16) is set to five different values from 1 to 1.5 bit/Sec/Hz, respectively. It can be seen that the proposed AO algorithm converges typically within six iterations. Specifically, the decreasing of the total power after four iterations is very small. Thus only a few iterations are required to achieve a good performance. This also indicates that the AO algorithm has a short processing delay, which is important for practical PLC relay systems. It can also be observed from Fig. 3 that with the increasing of averaged subchannel capacity, more transmission power is needed to meet the stricter QoS constraint, which reflects the typical QoS-cost tradeoff in communication systems.

Next, we compare the proposed AO power allocation algorithm on the general BMA relay scheme with the two-hop relay system as proposed in [4] and the BF relay system under the same channel conditions, and plot the total network power versus the common QoS requirements. We can see from Fig. 4 that the AO algorithm make the system meet the requirement with the least power consumption. The details of the power allocations on each subchannel for two-hop, BF and BMA relay systems has been shown in Fig. 5, where the averaged subchannel capacity is set to 1 bit/sec/Hz. Considering the the PLC system's possible electromagnetic interference (EMI) to the shortwave radio system, we hope this power saving property can relieve this issue to some extent.

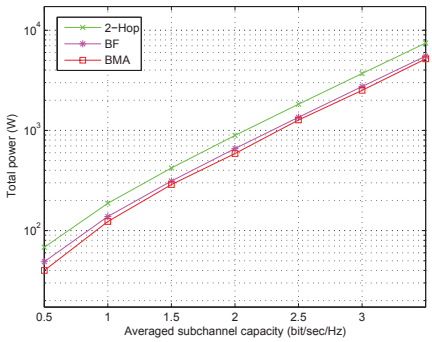

Fig. 4: Total power versus averaged subchannel capacity.

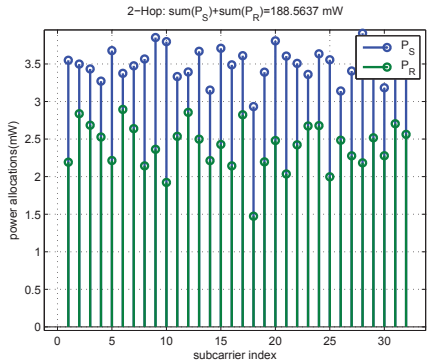

(a) Two-hop relay

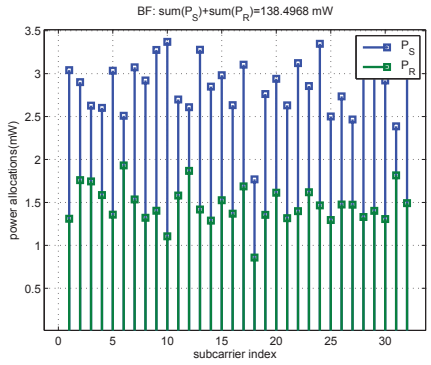

(b) Broadcast-and-forward (BF) relay

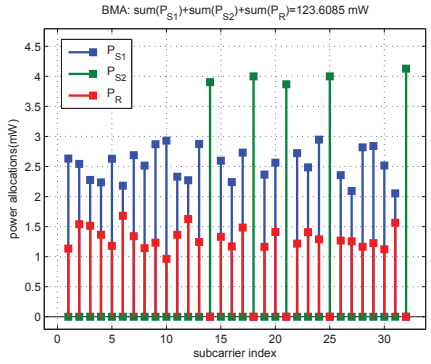

(c) broadcast-and-multiaccess (BMA) relay

Fig. 5: Power allocations on each subchannel of three relay schemes under the same channel conditions with common QoS requirement.

VIII. Conclusion

We have developed an iterative algorithm to jointly optimize the source power and relay power allocations for the general three-node/two-phase relay system, where the source transmits in both time-phases. Specifically, we examined the minimization of the total transmission power when there is a minimal channel capacity requirement from some indoor PLC system applications. Simulation results show that with respect to a two-hop and BF relay systems with certain QoS constraint, the proposed general relay system, along with the proposed alternative algorithm, can attain the same QoS requirement with less total transmission power.

References

[1] L. Lampe and A. J. Han Vinck, "Cooperative multihop power line communications," *IEEE the 16th International Symposium on Power-Line Communications and its Applications(ISPLC)*, Beijing, China, March 2012, pp. 1-6.

[2] A. M. Tonello, F. Versolatto, and S. D'Alessandro, "Opportunistic relaying in in-home PLC networks," *Proc. IEEE Global Telecommunications Conference (GLOBECOM'2010)*, Miami, FL, USA, Dec. 2010.

[3] L. Lampe, R. Schober, and S. Yiu, "Distributed space-time coding for multihop transmission in power line communication networks," *IEEE J. Sel. Areas Comm.*, vol. 24, pp. 1389-1400, Jul. 2006.

[4] W. Zhang, U. Mitra, and M. Chiang, "Optimization of amplify-and-forward multicarrier two-hop transmission," *IEEE Trans. Commun.* , vol. 59, pp. 1434-1445, May 2011.

[5] Y. Li, W. Wang, J. Kong, W. Hong, X. Zhang and M. Peng, "Power allocation and subcarrier pairing in OFDM-based relaying networks," *Proc. IEEE Int. Conference on Communications, 2008 (ICC '08)*, Beijing, China, May 2008, pp. 2602-2606.

[6] I. Hammerstrom and A. Wittneben, "On the optimal power allocation for nonregenerative OFDM relay links," *Proc. IEEE International Conference on Communications, 2006 (ICC '06)*, Istanbul, Turkey, June 2006, vol. 10, pp. 4463-4468.

[7] Y. Ma, A. Liu, and Y. Hua, "A dual-phase power allocation scheme for multicarrier relay system with direct link," *IEEE Trans. Signal Process.*, vol. 62, pp. 5-16, Jan. 2014.

[8] N. Papandreou and T. Antonakopoulos, "Bit and power allocation in constrained multicarrier systems: The single-user case," *EURASIP Journal on Advances in Signal Processing,* vol. 2008, Article ID 2008:643081.

[9] Y. Rong, X. Tang, and Y. Hua, "A unified framework for optimizing linear nonregenerative multicarrier MIMO relay communication systems," *IEEE Trans. Signal Process.*, vol. 57, pp. 4837-4851, Dec. 2009.

[10] F. J. Canete, J. A. C. Arrabal, L. Diez del Rio, and J. T. E. Munoz, "Analysis of the cyclic short-term variation of indoor power line channels," *IEEE J. Sel. Areas Comm.*, vol. 24, pp. 1327-1338, July 2006.

[11] F. J. Canete, J. A. Cortes, and L. Diez, "A channel model proposal for indoor power line communications," *IEEE Comm. Mag.* , vol. 49, pp. 166-174, Dec. 2011.

[12] D. Benyoucef, "A new statistical model of the noise power density spectrum for powerline communication," *IEEE the 7th International Symposium on Power-Line Communications and its Applications(ISPLC)*, Kyoto, Japan, March 2003, pp. 136-141.